**FACTA UNIVERSITATIS**
Series: **Mechanics, Automatic Control and Robotics** Vol.3, N° 13, 2003, pp. 657 - 669

# EVALUATION OF SMALL CRACK GROWTH MODELS FOR NOTCHED SPECIMEN UNDER AXIAL/TORSIONAL FATIGUE LOADING

*UDC 539.385 539.219.2*

**M. de Freitas, L. Reis, B. Li**

Departamento de Engenharia Mecânica, Instituto Superior Técnico,
Av. Rovisco Pais, 1049-001, Lisboa, Portugal
e-mail: mfreitas@dem.ist.utl.pt

**Abstract**. *Crack initiation and small crack growth behavior of notched specimens under various multiaxial loading paths are studied. Crack initiation and small crack growth were monitored by the replicas method. An improved model is proposed based on correcting the strain range parameter of the ASME code approach, taking into account the additional hardening caused by the non-proportional loading path, which accurately predict the fatigue lives for various non-proportional loading paths and provide an easy way to overcome the drawbacks of the current ASME code approach for non-proportional fatigue. Based on this corrected strain range parameters, a strain intensity factor range is used to correlating the experimental results of small crack growth rates and good correlation results are shown.*

**Key words**: *Multiaxial Fatigue, Small Crack Growth, Fatigue Life Prediction, Elastic-plastic Stress/Strain Behavior.*

## INTRODUCTION

Machine components and structures in service are generally subjected to multiaxial fatigue stress states, due to their complex geometrical shapes and/or complex loadings. Fatigue life evaluation of mechanical components under complex multiaxial fatigue conditions is of great importance to optimize structural design, and improve inspection and maintenance procedures [1].

Fatigue life generally consists of three stages: crack initiation, crack propagation and final fracture. For engineering design, crack initiation life is commonly defined as crack nucleation and small crack growth to NDT detectable crack size. Different mechanisms and controlling parameters dominate the fatigue life stages. A dominant fraction of total fatigue life may be spent in the growth of small cracks (less than approximately 1~2 mm). The problem of the nucleation and growth of small cracks has been conventionally

Received October 20, 2002

treated in the context of so-called fatigue crack initiation approaches, which are phenomenological stress-life and strain-life equations.

A new potentiality of assessing the fatigue strength and service life of structural component arises from small crack fracture mechanics. In recent years, substantial effort has been directed to model the small crack growth behavior [2-4], since an improved understanding of the ability to predict small crack growth behavior under multiaxial stress conditions would be very useful for fatigue design evaluations.

The objective of the present research is to study the local cyclic stress-strain responses, crack initiation and small crack growth behavior of notched specimen under cyclic bending/torsion loading, with various loading paths. Both experimental and numerical methods were used in the studies for two materials: the medium carbon steel, Ck45 and the high strength steel 42CrMo4.

## MATERIAL DATA, SPECIMEN FORM AND TEST PROCEDURE

The materials studied are the Ck45 steel in the normalized condition and the high strength steel 42CrMo4, quenched and tempered. The chemical compositions and mechanical properties are shown in tables 1 and 2, respectively.

Table 1. Chemical composition of Ck45 and 42CrMo4 steels (%)

| | C | Si | Mn | P | S | Cr | Ni | Mo | Cu |
|---|---|---|---|---|---|---|---|---|---|
| CK45 | 0.45 | 0.21 | 0.56 | 0.018 | 0.024 | 0.10 | 0.05 | 0.01 | 0.10 |
| 42CrMo4 | 0.39 | 0.17 | 0.77 | 0.025 | 0.020 | 1.10 | 0.30 | 0.16 | 0.21 |

The geometries and dimensions of the specimens used are shown in figure 1a, 1b. The specimens were machined from 25.0 mm diameter bars. After machining, some of the specimens were electro-polished, with the aim of taking away the residual stresses.

To study the effects of the loading paths on the additional hardening and fatigue damage, a series of loading paths were applied in the experiments as shown in table 3. The cyclic bending-steady torsion tests (case 0 in the table 3) were performed using the specimens of figure 1a) and a uniaxial 8500 Instron machine, and the remaining tests (cases 1-5 in the table 3) were performed using the specimens of figure 1b) and a biaxial 8800 Instron machine. Test conditions were as follows: frequency 12 Hz and room temperature in laboratory air. The detection of surface cracks was carried out by taking plastic replicas (15mm × 7mm) on point of maximum theoretical stresses, at regular intervals until 2~3mm of crack length. The observations of the plastic replicas were made using an optical microscope at a magnification between 50 and 1000 times.

**Table 2.** Mechanical properties of Ck45 and 42CrMo4 steels

| | | Ck45 | 42CrMo4 |
|---|---|---|---|
| Tensile strength | *Ru* (MPa) | 660 | 1100 |
| Yield strength | *Rp* 0.2, monotonic (MPa) | 410 | 980 |
| Elongation | *A* (%) | 23 | 16 |
| Young's modulus | *E* (GPa) | 206 | 206 |
| Hardness | *HV* | 195 | 362 |

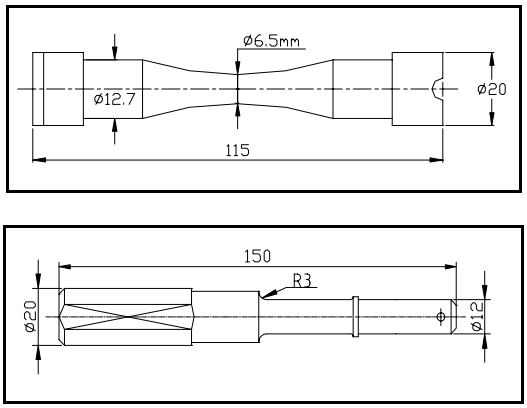


Fig. 1a, 1b. Geometries and dimensions of the specimens

Table 3. Multiaxial fatigue loading paths

| | |
|---|---|
| 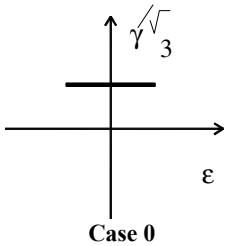  **Case 0** | 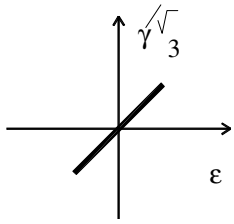  **Case 1** |
| 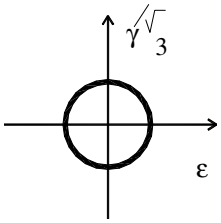  **Case 2** | 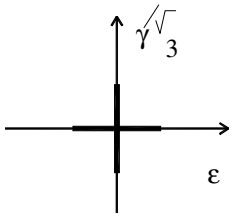  **Case 3** |
| 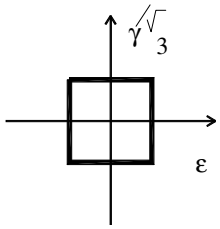  **Case 4** | 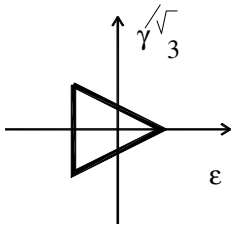  **Case 5** |

## CYCLIC STRESS-STRAIN RESPONSES

When an elastic-plastic material is subjected to cyclic loading, the stress and strain history will initially go through a transient state which asymptotes to a cyclic state. In this cyclic state, the behavior of the body can be characterized by four alternative modes of behaviors [5]: 1. Elastic region. 2. Elastic shakedown. 3. Plastic shakedown. 4. Ratcheting.

Modeling the cyclic behavior of a material subjected to multiaxial elasto-plastic deformation is essential for predicting the fatigue life of components using multiaxial fatigue criteria. Because local yielding may occur at notches and other stress concentrations, in spite of that the global component responds elastically.

To study the cyclic stress-strain behavior of the materials, low cycle fatigue tests were carried out using a biaxial hydraulic machine (8800 Instron). All the cyclic tests were fully reversed ($R = -1$, axial strain controlled), at a frequency of 0.2 Hz and performed at room temperature.

The cyclic stress-strain curve is obtained by connecting the tips of stable hysteresis loops for different strain amplitudes of fully reversed strain-controlled tests as shown in the Ramberg-Osgood relationship:

$$\frac{\Delta\varepsilon}{2} = \frac{\Delta\sigma}{2E} + \left(\frac{\Delta\sigma}{2K'}\right)^{1/n'} \tag{1}$$

For 'Masing-type' materials, the hysteresis loop curves can be described by the cyclic stress-strain curve Eq.(1) magnified by a factor of 2:

$$\Delta\varepsilon = \frac{\Delta\sigma}{E} + 2\left(\frac{\Delta\sigma}{2K'}\right)^{1/n'} \tag{2}$$

As an easy engineering approach, the Masing curve of Eq. (2) is popularly used. If the material has a 'non-Masing' behavior, the master curve approach should be used, as described in Ref. [6].

The cyclic properties obtained from fitting the test results are shown in Table 4.

Table 4. Cyclic properties of Ck45 and 42CrMo4 steels ($f = 0.2\text{s}^{-1}$)

| | | CK45 | 42CrMo4 |
|---|---|---|---|
| Yield strength | $Rp_{,0.2}$,cyclic (MPa) | 240 | 540 |
| Strength coefficient | $K'$(MPa) | 1206 | 1420 |
| Strain hardening exponent | $n'$ | 0.20 | 0.12 |
| Fatigue strength coefficient | $\sigma_f'$(MPa) | 948 | 1154 |
| Fatigue strength exponent | b | –0.102 | –0.061 |
| Fatigue ductility coefficient | $\varepsilon_f'$ | 0.17 | 0.18 |
| Fatigue ductility exponent | $c$ | –0.44 | –0.53 |

## MULTIAXIAL FATIGUE MODELS FOR CRACK INITIATION LIFE PREDICTION

Many multiaxial fatigue models have been proposed to reduce the complex multiaxial stress/strain state into an equivalent uniaxial condition. Some selected models are briefly reviewed as following:

**Von Mises Criterion**

The maximum octahedral shear strain amplitude is one of the most common methods, where $\varepsilon_{i,a}$ denotes principal strain amplitude and $\nu$ is the Poisson's ratio.

$$\varepsilon_{eq,a} = \frac{1}{(1+v)\sqrt{2}}\{(\varepsilon_{1,a}-\varepsilon_{2,a})^2+(\varepsilon_{2,a}-\varepsilon_{3,a})^2+(\varepsilon_{3,a}-\varepsilon_{1,a})^2\}^{1/2} \tag{3}$$

Eq.(3) gives the same equivalent strain amplitude for both in- and out-of-phase strain histories. Some experimental results contradict this prediction; it has been shown that the fatigue life under out-of-phase loading condition is lower than fatigue life under in-phase loading at the same applied strain amplitudes.

**ASME Code**

The ASME Code Case N-47-23 [7] is based on the von Mises hypothesis, but employs the strain difference $\Delta\varepsilon_i$ between time $t_1$ and $t_2$, where the equivalent strain range $\Delta\varepsilon_{eq}$ is maximized with respect to time.

$$\begin{aligned}\varepsilon_{eq,a} = \frac{1}{(1+v)\sqrt{2}}\{&(\Delta\varepsilon_x-\Delta\varepsilon_y)^2+(\Delta\varepsilon_y-\Delta\varepsilon_z)^2+(\Delta\varepsilon_z-\Delta\varepsilon_x)^2+\\ &+6(\Delta\varepsilon_{xy}{}^2+\Delta\varepsilon_{yz}{}^2+\Delta\varepsilon_{xz}{}^2)\}^{1/2}\end{aligned} \tag{4}$$

Eq. (4) gives a lower equivalent strain range for out-of-phase loading than the in-phase loading, which estimates unconservative life for non-proportional fatigue.

**Critical Plane Models**

During the past 20 years, the critical plane approaches for predicting life to crack initiation have been developed and applied for multiaxial fatigue problems. All the theories based on this approach define a critical plane on which maximum damage should occur and thus specify the plane of crack initiation and growth.

The tensile damage model proposed by Smith, Watson and Topper [8] is formulated as:

$$\frac{\Delta\varepsilon_{\max}\sigma_{\max}}{2} = \frac{(\sigma_f')^2}{E}(2N_f)^{2b}+\varepsilon_f'\sigma_f'(2N_f)^{b+c} \tag{5}$$

where $\Delta\varepsilon_{max}/2$ is the maximum normal strain amplitude, $\sigma_{max}$ is the maximum normal stress on the $\Delta\varepsilon_{max}$ plane, $E$ is the young's modulus, $\sigma_f'$ is the fatigue strength coefficient, $\varepsilon_f'$ is the fatigue ductility coefficient, and $b$ and $c$ are fatigue strength and fatigue ductility exponents, respectively.

The shear damage model proposed by Fatemi and Socie [9] has been found to be superior for materials whose damage development is shear dominated:

$$\frac{\Delta\gamma_{\max}}{2} = \left(1+k\frac{\sigma_{n,\max}}{\sigma_y}\right) = \frac{\tau_f'}{G}(2N_f)^{b_0}+\gamma_f'(2N_f)^{c_0} \tag{6}$$

where $\Delta\gamma_{max}/2$ is the maximum shear strain amplitude, $\sigma_{n,max}$ is the maximum normal stress on the $\Delta\gamma_{max}$ plane, $\sigma_y$ is the material monotonic yield strength, $k$ is a material constant, which can be found by fitting fatigue data from simple uniaxial tests to fatigue data from simple torsion tests. $G$ is the shear modulus, $\tau_f'$ is the shear fatigue strength coefficient, $\gamma_f'$ is the shear fatigue ductility coefficient, and $b_0$ and $c_0$ are shear fatigue strength and shear fatigue ductility exponents, respectively. These properties can be obtained from torsion fatigue test, or they can be estimated from uniaxial strain-life properties as $\tau_f' \approx \sigma_f'/\sqrt{3}$, $b_0 \approx b$, $\gamma_f' \approx \sqrt{3}\varepsilon_f'$ and $c_0 \approx c$.

For non-proportional multiaxial loading condition with rotating principal directions, a new definition of the critical plane is the plane with the maximum value of the damage parameter $\left[\frac{\Delta\gamma}{2}\left(1+k\frac{\sigma_{n,max}}{\sigma_y}\right)\right]_{max}$ instead of that with the maximum shear strain amplitude $\Delta\gamma_{max}$ [1].

**An Improved Model Based on the ASME Code**

The ASME Code approach expressed in Eq. (4), define a parameter which has a drawback that is, it produces a lower equivalent strain range for out-of-phase than the in-phase loading, which estimates unconservative life for non-proportional fatigue.

In this paper, an improved model based on the ASME code approach is proposed by considering the additional hardening and correcting the strain range parameter for non-proportional loading path:

$$\Delta\varepsilon_{NP} = (1+\alpha F_{NP})\Delta\varepsilon_{eq} \tag{7}$$

where $F_{NP}$ is the non-proportionality factor of the loading path, $\alpha$ is a material constant of additional hardening, $\Delta\varepsilon_{eq}$ is the strain range parameter calculated by Eq. (4), and $\Delta\varepsilon_{NP}$ is the corrected strain range parameter.

Eq. (7) is similar with the approach proposed by Itoh et al. [10], but here the MCE (Minimum Circumscribed Ellipse) approach previously developed by the authors [11] is applied for evaluating the non-proportionality factor $F_{NP}$ of the loading path, defined as the ratio between the minimum radius to the maximum radius of the ellipse circumscribing the shear path [11].

Then the Manson-Coffin formulation can be used for life predictions:

$$\frac{\Delta\varepsilon_{NP}}{2} = \frac{\sigma_f' - \sigma_m}{E}(2N_f)^b + \varepsilon_f'(2N_f)^c \tag{8}$$

where $\sigma_m$ is the mean stress, and the other terms have the same definitions in the Eq.(5).

In this paper, the Eq.(7-8) are applied for correlating the test fatigue life results.

## SMALL CRACK GROWTH MODELS IN MULTIAXIAL FATIGUE

As described in the above section, the so-called fatigue crack initiation approaches are phenomenological stress-life and strain-life equations. On the other hand, the crack propagation mechanisms are often analysed using linear elastic fracture mechanics

(LEFM) approach. The stress intensity factor is extensively used to evaluate crack propagation under Mode I loading condition.

For mixed-mode loading, the fatigue crack growth rate also may be expressed by the Paris law where the stress intensity factor range is replaced by an equivalent stress intensity factor range $\Delta K_{eq}$:

$$\frac{da}{dN} = C(\Delta K_{eq})^m \tag{9}$$

There are many approaches proposed to define the equivalent stress intensity factor range $\Delta K_{eq}$ for mixed-mode loadings, however, no universally accepted approach exists. One of them was proposed by Hua [12] based on the addition of the Irwin´s elastic energy release rate parameters [13] for the three loading modes:

$$\Delta K_{eq} = (G_{total} E)^{1/2} = [\Delta K_I^2 + \Delta K_{II}^2 + (1+\nu)\Delta K_{III}^2]^{1/2} \tag{10}$$

where

$$\Delta K_I = Y_1 \Delta\sigma(\pi a)^{1/2} \tag{11}$$

$$\Delta K_{II} = Y_2 \Delta\tau(\pi a)^{1/2} \tag{12}$$

$$\Delta K_{III} = Y_3 \Delta\tau(\pi a)^{1/2} \tag{13}$$

and $Y_1$, $Y_2$, $Y_3$ are geometry factors which are functions of the crack aspect ratio, Poisson´s ratio, the parametric angle defining the point at the crack line, and loading conditions.

For axial-torsional fatigue crack growth (Modes I and II), Eq. (10) becomes:

$$\Delta K_{eq} = (G_{total} E)^{1/2} = [\Delta K_I^2 + \Delta K_{II}^2]^{1/2} \tag{14}$$

However, the stress intensity factor $K$ can only be used in the cases where the plastic zone size at the crack tip is small and cannot be used for the analysis of short fatigue crack growth, where the elastic-plastic loading conditions are significant.

For elastic-plastic loading conditions, a strain intensity factor, $\Delta K_I(\varepsilon)$, is often used as shown in Ref. [1]. Any of the equivalent stress intensity models, such as Eq. (14), could be used as strain intensity models with the appropriate substitution of $E\Delta\varepsilon$ or $G\Delta\gamma$ for the stress terms. This allows an effective strain intensity factor, $\Delta K_{eq}(\varepsilon)$, to be written in terms of the strain amplitudes and crack geometry factors for Mode I and Mode II, $Y_1$ and $Y_2$. Eq. (14) can be expressed as:

$$\Delta K_{eq}(\varepsilon) = \left[ (Y_1 E\Delta\varepsilon)^2 + \left( Y_2 \frac{E}{2(1+\nu)} \Delta\gamma \right)^2 \right]^{1/2} \sqrt{\pi a} \tag{15}$$

where $\Delta\varepsilon$ and $\Delta\gamma$ are the normal and shear strain ranges on the crack plane including both the elastic and plastic components.

The fatigue damage parameter given by the left-hand side of Eq. (6) had been shown to be representative of the damage mechanism and accumulation under a wide variety of multiaxial loading conditions, it is postulated that it can represent the driving force for crack propagation. Therefore, Reddy and Fatemi [4] proposed the extension of this

parameter as a measure of crack growth rate in the form of an effective strain-based intensity factor range:

$$\Delta K_{CPA} = G\Delta\gamma_{\max}(1 + k\,\sigma_n^{\max}/\sigma_y)\sqrt{\pi a} \tag{16}$$

As $\Delta K_{eq}$ in Eq.(9), $\Delta K_{CPA}$ is related to multiaxial fatigue crack growth rate data by the same type of power law relation:

$$\frac{da}{dN} = C(\Delta K_{CPA})^m \tag{17}$$

where $C$ and $m$ are material dependent constants, but with values different from those in Eq. (9).

Similar to Eq. (16), the Eq. (7) can also be extended as a measure of crack growth rate in the form of an effective strain-based intensity factor range:

$$\Delta K_{NP} = E(1 + \alpha F_{NP})\Delta\varepsilon_{eq}\sqrt{\pi a} \tag{18}$$

In this paper, Eq.(18) is applied for correlating the small crack growth rates.

## FEM BASED PROCEDURE FOR MULTIAXIAL FATIGUE LIFE PREDICTION

For non-proportional multiaxial loading condition with rotating principal directions, a new definition of the critical plane is the plane with the maximum value of the damage parameter $\left[\frac{\Delta\gamma}{2}\left(1 + k\frac{\sigma_{n,\max}}{\sigma_y}\right)\right]_{\max}$ instead of that with the maximum shear strain amplitude $\Delta\gamma_{\max}$ [1].

The critical damage models of Eqs.(5) and (6), and the improved ASME code approach of Eqs.(7) and (8) are incorporated into the life prediction procedure of this paper. For a general multiaxial fatigue life assessment of engineering components, both tensile and shear failure modes should be considered in the computation procedure reflecting the two possible modes of cracking [8].

The FEM based multiaxial fatigue life prediction procedure is implemented as follows: 1. Elastic finite element analyses for the component with coarse FE mesh, identify the critical locations with high peak stresses under combined loading. Calculate the stress concentration factors. 2. Refine the FE mesh at the critical locations and carry out elastic-plastic FEA. 3. Obtain time histories of the strain tensor (elastic and plastic strain components) and stress tensor at the critical location under consideration from the results of FEA. 4. For a surface element, the strains and stresses can be transformed into the shear strain (stress) and normal strain (stress) acting on a plane $\theta$. 5. Calculate the normal strain range $\Delta\varepsilon$, shear strain range $\Delta\gamma$ and normal stress $\sigma_n$ for each plane $\theta$. 6. Search the plane $\theta_1^*$ with the maximum tensile damage parameter: $d_t = \max_{\theta}\{\Delta\varepsilon\sigma_n/2\}$. 7. Solve for fatigue life $N_{ft}$ from the tensile damage model of Eq.(5): $d_t = \frac{(\sigma_f')^2}{E}(2N_{ft})^{2b} + \varepsilon_f'\sigma_f'(2N_{ft})^{b+c}$. The Newton-Raphson (N-R) method is used for iterative solution of $N_{ft}$. The initial guess for the N-R method is obtained as follows: (a) calculate $N_{ft}$ with the first term on the right hand side discarded; (b) calculate $N_{ft}$ with the second term on the right hand side dis-

carded; (c) take the larger value from (a) or (b) as the initial guess. 8- Search the plane $\theta_2^*$ with the maximum shear damage parameter: $d_s = \max_{\theta}\left\{\left[\frac{\Delta\gamma}{2}\left(1+k\frac{\sigma_{n,\max}}{\sigma_y}\right)\right]\right\}$. 9. Solve for fatigue life $N_{fs}$ from the shear damage model of Eq.(6): $d_s = \frac{\tau'_f}{G}(2N_{fs})^{b_0} + \gamma'_f(2N_{fs})^{c_0}$. The Newton-Raphson (N-R) method is used for iterative solution of $N_{fs}$. The initial guess is obtained with the same method in the step 7. 10. Take the smaller of the two values, $N_{ft}$ and $N_{fs}$, as the fatigue life estimate of the component.

## RESULTS AND DISCUSSIONS

The FEM based multiaxial fatigue life prediction procedures were applied to the notched shaft specimen subjected to combined bending and torsion loadings.

Isoparametric solid elements with 20 nodes were used. For elastic solutions, a course mesh with 784 elements and 3705 nodes were used. For elastic-plastic FEA, the mesh was refined to be with 1372 elements and 6297 nodes. Kinematic hardening model with von Mises yield criterion and associative flow rule was used for elastic-plastic FEA.

### Calculated local stress-strain

The FEA ABAQUS calculated stress-strain results, are shown on fig. 2, where are also presented the results of the equivalent stresses and strains calculated by the approximated methods (Neuber and Glinka) generally used for uniaxial loading cases. It is to be remarked that both Glinka and Neuber methods were originally applied to uniaxial loading, but here the application is made to multiaxial loading. This comparison shows that the Glinka method predicts less equivalent plastic strain than the Neuber rule for equivalent loading cases. The calculated equivalent plastic strain by FEA ABAQUS lay between the two predictions methods.

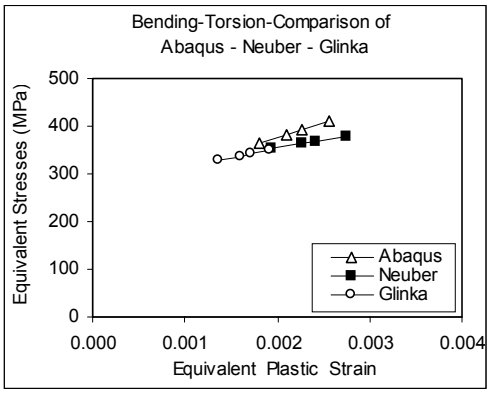


Fig. 2. Comparison of results (Case 0)

## CRACK INITIATION ON NOTCHED SPECIMENS / SMALL CRACK GROWTH

The replication method, described before, was used to monitor the crack initiation on the notched specimens subjected to multiaxial loading (cyclic bending + steady torque). This method with an optical microscopy allows the detection of very short cracks. In this study, the life spent to a crack attain a value of 0.1mm crack length will be consider as crack initiation. An example of the observed cracks through this method is shown on fig. 3 and fig. 4. Several cracks usually appeared on each specimen with one of them later

becoming the most prominent. Meanwhile, it is for higher applied stresses (both bending and torsion) that more cracks are observed at crack initiation, as shown in fig.3 and compared with fig. 4, where only one crack was visible due to a lower cyclic bending stress. Linking of cracks sometimes leads to a sudden increase in their surface length. This usually grew to be the failure crack. Once monitored the crack initiation, it is possible to measure the replicas and with these data to evaluate the crack growth rate of the crack. In figures 5 and 6, for two levels of loading, an example of measured crack lengths are plotted versus the number of cycles.

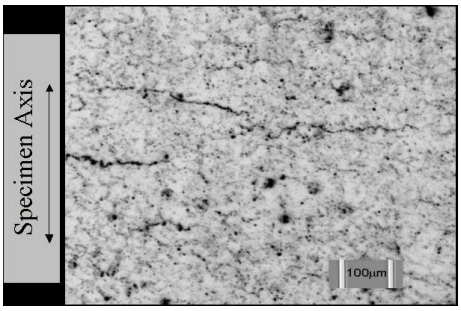


Fig. 3. Plastic replica with several cracks

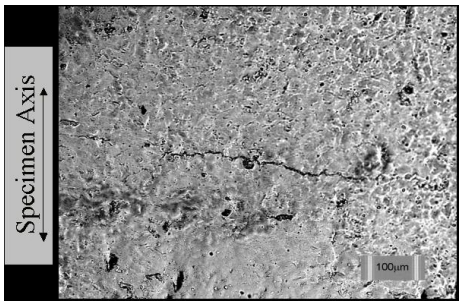


Fig. 4. Plastic replica with one crack

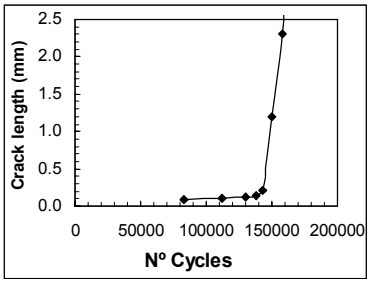


Fig. 5. Measured crack length versus applied cycles for CK45 (Case 0)

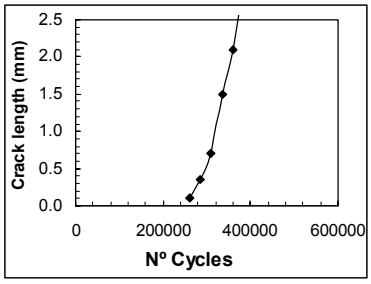


Fig. 6. Measured crack length versus applied cycles for CK45 (Case 0)

**Comparison of predicted and experimental crack initiation lives**

*Loading path 0*

Crack initiation lives of notched specimens of Ck45 steel subjected to biaxial loading (cyclic bending + steady torque, case 0 in table 3) were predicted with the life prediction procedure described in the above section. The local stress-strain history results calculated by FEA ABAQUS were applied for the life predictions. Fig. 7 shows the comparison of the experimental fatigue life against the predicted results using the ASME code approach of Eq. (4) and the Fatemi-Socie parameter of Eq.(6), respectively. The results show that the Fatemi-Socie parameter gives better correlation with experimental results than the ASME method for this material and loading case.

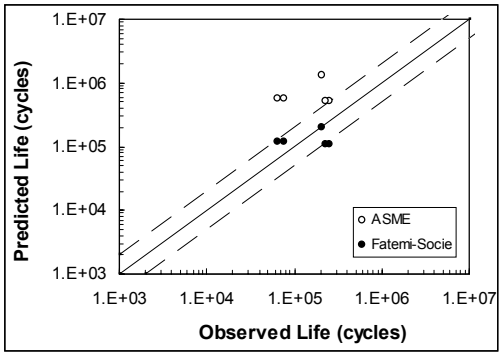


Fig. 7. Comparison of experimental fatigue life with predicted results by ASME method's and Fatemi Socie method's (Loading Path 0)

*Loading paths 1 to 5*

The crack initiation lives of the specimens of 42CrMo4 steel subjected to various loading paths (cases 1 to 5 in table 3) were predicted with the improved ASME code approach of Eqs.(7-8). For 42CrMo4 steel, the material constant of additional hardening $\alpha$ is 0.188 as correlated from experimental results by Chen et al [14]. The non-proportionality factor $F_{NP}$ is calculated for each loading path by the MCE approach as described in detail in Ref.[11]. For each loading path shown in the table 3, a minimum circumscribed ellipse is found to enclose the strain path, then the non-proportionality factor $F_{NP}$ is calculated as $F_{NP} = R_b / R_a$, where $R_b$ and $R_a$ are the minor and major radius of the ellipse, respectively.

Fig. 8 shows the comparisons of the experimental fatigue life against the predicted results. It is shown that the predictions have good accuracy by comparison with experimental results, where the dashed lines represent the error band of factor 2.

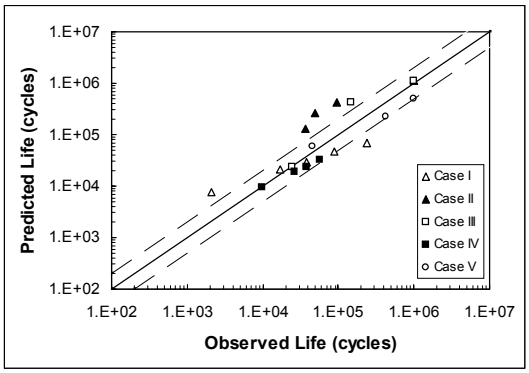


Fig. 8. Comparison of experimental fatigue life with predicted results by Improved ASME method's (Loading Paths from case 1 to 5)

**Correlation of the Small Crack Growth Rate with Strain Intensity Factor Range**

The measured crack growth rate shown in Figs. 5 and 6 are correlated by the Strain Intensity Factor Range expressed in Eq.(18). The correlated *C* and *m* parameters are 1.E-18 and 13.111, respectively. Fig. 9 shows that the crack growth rate can be correlated well by the Strain Intensity Factor Range expressed in Eq.(18), which is proposed in this paper.

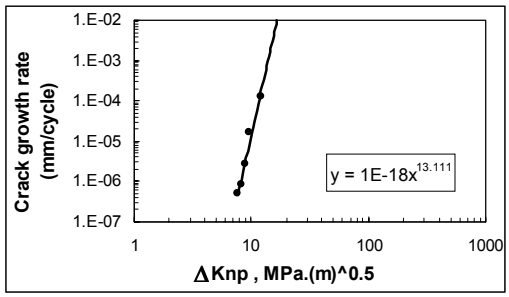


Fig. 9. Correlation of crack growth rate with strain intensity factor range

## CONCLUSIONS

1. Replica method allows a good monitoring of crack initiation lives and small crack growth rates under multiaxial fatigue loading conditions.
2. Neuber and Glinka methods give acceptable estimations of local equivalent plastic strain at notches for biaxial loading when compared with FE analysis.
3. The proposed approach based on correcting the strain range parameter of the ASME code approach, taking into account the additional hardening caused by the non-proportional loading path, can predict the fatigue lives well for various non-proportional loading paths. This proposal provides an easy way to overcome the drawbacks of the current ASME code approach.
4. The proposed strain intensity factor range based on the corrected strain range parameters gives a good correlation for the experimental small crack growth rates.

**Acknowledgements**. *Financial support from the Fundação para Ciência e Tecnologia (FCT) is acknowledged.*

## REFERENCES

1. Socie, D. F. and Marquis, G. B. (2000) "Multiaxial Fatigue", Society of Automotive Engineers, Warrendale, PA 15096-0001.
2. Park, J., Nelson, D. and Rostami, A. (2001) "Small Crack Growth in Combined Bending-torsion Fatigue of A533B Steel," *Fatigue Fract. Engng Mater Struct*, **24**, pp.179-191.
3. McDowell, D.L. and Bennett, V.P. (1996) "Small Crack Growth in Combined Bending-torsion Fatigue of A533B Steel," *Fatigue Fract. Engng Mater Struct*, **19**, pp.821-837.
4. Reddy, S.C. and Fatemi, A. (1992) "Small Crack Growth in Multiaxial Fatigue," Advances in Fatigue Lifetime Predictive Techniques, ASTM STP 1122, M.R. Mitchell and R.W. Landgraf, Eds., American Society for Testing and Materials, Philadelphia, pp.276-298.
5. Ponter, A.R.S. and Carter, K.F., *Comput. Methods Appl. Mech. Engrg.,* **140**, 1997, pp. 259-279.
6. Ellyin,F., *Fatigue Damage*, *Crack Growth and Life Prediction*, Chapman & Hall, 1997.

7. ASME Code Case N-47-23 (1988) Case of ASME Boiler and Pressure Vessel Code, American Society of Mechanical Engineers.
8. Smith, R.N., Watson, P. and Topper, T.H., *J. of Materials*, **5**(4), 1970, pp. 767-778.
9. Fatemi, A. and Socie, *Fatigue and Fract. of Engin. Mater. and Struct.*, **11**(3), 1988, pp.149-165.
10. Itoh, T. and Miyazaki, T. (2001) "A damage model for estimating low cycle fatigue lives under non-proportional multiaxial loading", *Proceedings of the 6th International Conference on Biaxial/Multiaxial Fatigue & Fracture*, Edited by M. de Freitas, Lisbon, June 25-28, pp. 503-510.
11. M.de Freitas, B. Li and J.L.T. Santos (2000) Multiaxial Fatigue and Deformation: Testing and Prediction, ASTM STP 1387, S. Kaluri and P.J. Bonacuse, Eds., American Society for *Testing and Materials, West Conshohocken, PA, pp.139-156.*
12. Hua, C. T. (1984) "Fatigue Damage and Small Crack Growth During Biaxial Loading", Ph. D. dissertation, Department of Mechanical and Industrial Engineering, University of Illinois at Urbana-Champaign.
13. Irwin, G. R. (1967) "Fracture Mechanics Applied to Adhesive Systems", in Treatise on Adhesion and Adhesives, Vol. 1, R.L. Patrik, Ed., Marcel Dekker, New York, pp. 233-267.
14. Chen, X., Gao Q. and Sun, X.F. (1996) "Low-Cycle Fatigue Under Non-proportional Loading", *Fatigue Fract. Engng Mater Struct*, **19**, No. 7, pp.839-854.

# ODREDJIVANJE MODELA NAPREDOVANJA MALIH PRSLINA ZA ZAREZANE UZORKE POD OSNO/TORZIONIM OPTEREĆENJEM ZAMOROM

**M. de Freitas, L. Reis, B. Li**

*Proučeno je zapodinjanje prsline i ponašanje napredovanja male prsline zarezanih uzoraka po različitim multiaksijalnim putanjama opterećenja. Zapodinjanje prsline i napredovanje male prsline monitorovani su metodom replika. Predlaže se unapredjeni model koji se zasniva na ispravljanju parametra opsega dilatacije iz ASME kod pristupa, pri čemu se ima u vidu dodatno otvrdnjavanje koje je uzrokovano neproporcionalnom putanjom opterećenja, što sa tačnošću predvidja trajanje pri zamoru različitih neproporcionalnih putanja opterećenja i pruža jednostavan način za prevazilaženje loše strane trenutnog ASME kod pristupa za neproporcionalni zamor. Na osnovu prepravljenih parametara opsega dilatacije koristi se opseg faktora intenziteta dilatacije u odnosu na eksperimentalne rezultate stopa napredovanja malih prslina, i prikazani su valjani rezultati korelacije.*